Acta Crystallographica Section D
Biological Crystallography
ISSN 0907-4449

The atomic resolution structure of methanol dehydrogenase from *Methylobacterium extorquens*

P. A. Williams, L. Coates, F. Mohammed, R. Gill, P. T. Erskine, A. Coker, S. P. Wood, C. Anthony and J. B. Cooper*

School of Biological Sciences, University of Southampton, Bassett Crescent East, Southampton SO16 7PX, England

Correspondence e-mail: j.b.cooper@soton.ac.uk

Received 1 September 2004
Accepted 23 October 2004

PDB Reference: methanol dehydrogenase, 1w6s, r1w6ssf.

The crystal structure of methanol dehydrogenase (MDH) from *Methylobacterium extorquens* has been refined without stereochemical restraints at a resolution of 1.2 Å. The high-resolution data have defined the conformation of the tricyclic pyrroloquinoline quinone (PQQ) cofactor ring as entirely planar. The detailed definition of the active-site geometry has shown many features that are similar to the quinohaemoprotein alcohol dehydrogenases from *Comamonas testosteroni* and *Pseudomonas putida*, both of which possess MDH-like and cytochrome *c*-like domains. Conserved features between the two types of PQQ-containing enzyme suggest a common pathway for electron transfer between MDH and its physiological electron acceptor cytochrome c_L. A pathway for proton transfer from the active site to the bulk solvent is also suggested.

1. Introduction

Methanol dehydrogenase (MDH) is a pyrroloquinoline quinone-containing protein found in the periplasm of many Gram-negative bacteria. This enzyme, which oxidizes methanol to formaldehyde, participates in a short electron-transfer chain (Anthony, 1992, 2004). The reduced pyrroloquinoline quinone (PQQ) transfers two electrons in single electron-transfer steps to cytochrome c_L, creating a semiquinone form of the prosthetic group after the first electron transfer (Dijkstra *et al.*, 1989). Cytochrome c_L is subsequently oxidized by a small class I *c*-type cytochrome, cytochrome c_H (Read *et al.*, 1999), which is in turn oxidized by the membrane oxidase cytochrome aa_3. This pathway produces a proton motive force sufficient to drive the production of just under one molecule of ATP per molecule of methanol oxidized.

MDH is a large tetrameric protein with an $\alpha_2\beta_2$ subunit composition. The large α-subunit (66 kDa) consists of a single domain with a β-propeller fold. The propeller fold is composed of eight four-stranded β-sheets arranged about an eightfold pseudosymmetry axis; PQQ is situated at the centre of the molecule on the eightfold pseudosymmetry axis (Fig. 1). This β-propeller fold has been identified in an increasing number of unrelated proteins, with a range of four to eight 'propeller blades'. In the case of MDH the propeller fold is stabilized by regularly spaced tryptophan residues, which form hydrophobic and polar interactions with residues in the same and in adjacent β-sheets; this arrangement is termed the tryptophan-docking motif (Ghosh *et al.*, 1995). The smaller β-subunit (8 kDa) forms a mainly α-helical structure, which wraps around the outside of the α-subunit (Fig. 1), although it is not obvious what (if any) function it serves.

The α-subunit harbours the active site, which consists of the PQQ prosthetic group, a calcium ion and the catalytic amino

acid Asp303 (Afolabi *et al.*, 2001). As shown in Fig. 2, PQQ forms many hydrogen bonds to protein atoms in the active site and also provides three of the six atoms coordinated to the calcium ion. In addition to these polar interactions, PQQ forms hydrophobic contacts with a vicinal disulfide bond formed between two adjacent cysteines (Cys103 and Cys104) and the indole ring of Trp243.

The structure of MDH has been solved previously from the bacteria *Methylobacterium extorquens* and *Methylophilus methylotrophus* W3A1 to a resolution of 1.94 and 1.90 Å, respectively (Ghosh *et al.*, 1995; Xia *et al.*, 1999). In both of these analyses there appeared to be uncertainty over the conformation of PQQ, in particular the orthoquinone moiety (Fig. 2) formed by the two O-atom substituents of the central six-membered ring. The structure from *Mb. extorquens* suggested that the C-4 carbonyl atom was not in the expected planar conformation but instead exhibited a distortion from the plane of the ring towards the Trp243 indole ring. In contrast, the structure of MDH from *Mp. methylotrophus* showed that the C-5 atom was in a tetrahedral conformation, causing the C-5 atom to be raised above the PQQ tricyclic plane towards the vicinal disulfide bridge.

In this communication, we present an atomic resolution structure of MDH refined to 1.2 Å from the facultative methylotroph *Mb. extorquens*. The high-resolution X-ray diffraction data allowed the structure to be refined with anisotropic *B* factors and without any restraints imposed on the protein or the prosthetic group. Under these refinement conditions, the tricyclic ring of the PQQ prosthetic group is planar. The higher accuracy of the 1.2 Å resolution structure has led us to revise the coordination geometry of the active-site calcium ion. Finally, the high resolution of the data set has allowed an extensive comparison of the active-site composition with that of the quinohaemoprotein alcohol dehydrogenases from *Comamonas testosteroni* (Oubrie *et al.*, 2002) and *Pseudomonas putida* (Chen *et al.*, 2002). This has allowed putative electron- and proton-transfer routes from PQQ to the soluble cytochrome electron acceptor and periplasm, respectively, to be postulated.

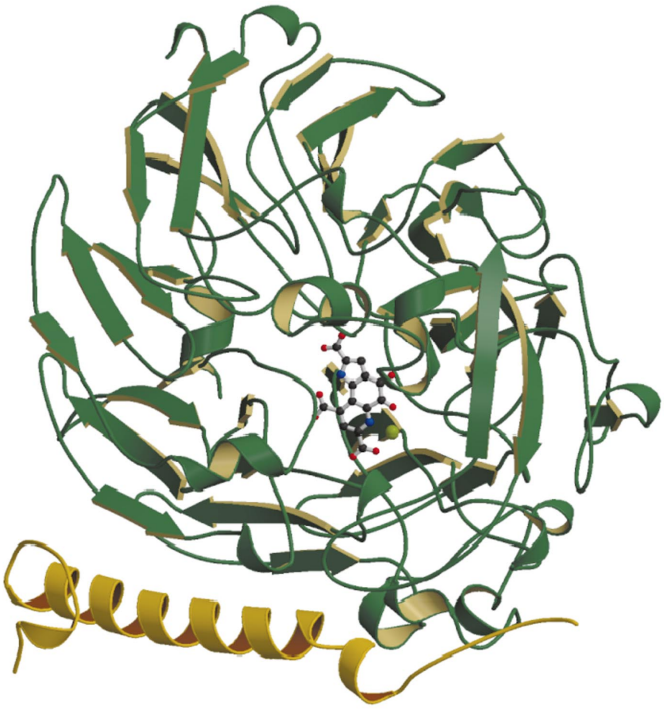

Figure 1
An $\alpha\beta$ unit from methanol dehydrogenase. The large α-subunit (shown in green) is folded into a β-propeller structure, with the PQQ prosthetic group and calcium ion (green sphere) at the centre of this fold; the small β-subunit (yellow) wraps around the side of the α-subunit.

2. Materials and methods

2.1. Protein crystallization

The methanol dehydrogenase crystals were grown by the hanging-drop vapour-diffusion method, in which 3 µl volumes of 15 mg ml^{-1} protein solution at pH 8.0 in 20 m*M* Tris buffer were placed on siliconized cover slips and then mixed with equal volumes of the well solution. Each cover slip was then sealed with high-vacuum grease over a well containing 1 ml 20% PEG 8000 pH 9.0. Large crystals appeared after two weeks.

2.2. Data collection and refinement

Diffraction data were collected at the ESRF, Grenoble (beamline ID-29). A high-resolution pass of 185° was collected

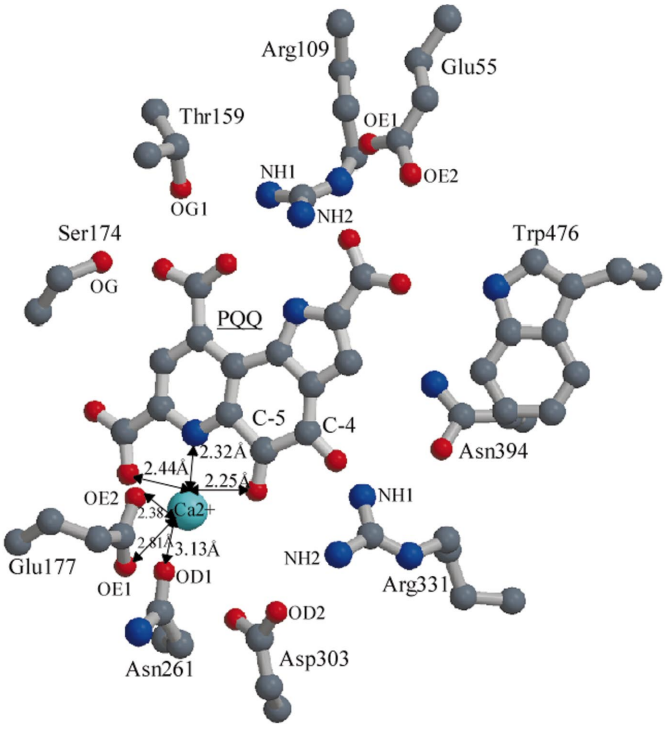

Figure 2
The equatorial interactions of PQQ in the active site and the dative bonds that coordinate the calcium. The lengths of the bonds to the Ca^{2+} ion are all between 2.4 and 2.8 Å. The orthoquinone group is formed by the central six-membered ring with two O-atom substituents. The vicinal disulfide bond formed by cysteines 103 and 104, which packs against the PQQ ring, has been omitted for clarity.

with an oscillation angle of 1° and a crystal-to-detector distance of 100 mm. A low-resolution pass of 185° was also collected with the same oscillation angle and crystal-to-detector distance using an attenuated beam and shorter exposures in an effort to measure reflections that might have been overloaded in the high-resolution pass. The crystals were found to belong to the triclinic space group $P1$ and have unit-cell parameters $a = 61.0$, $b = 71.7$, $c = 85.6$ Å, $\alpha = 86.2$, $\beta = 104.4$, $\gamma = 109.9°$. The data were processed using *MOSFLM* (Leslie, 1992) and scaled with *SCALA* (Collaborative Computational Project, Number 4, 1994). The resulting data set contained 373 341 unique reflections with an $R_{\rm merge}$ of 10.3%. A set of reflections representing 5% of the unique data was chosen at random for inclusion in an $R_{\rm free}$ set (Brünger, 1992). The program *MOLREP* (Vagin & Teplyakov, 1997) was used to obtain initial phases. The search model was an $\alpha_2\beta_2$ tetramer from a previously solved MDH structure (Afolabi *et al.*, 2001) with the PQQ cofactor and metal ions removed. Two significant peaks of 47.45σ and 47.21σ, which corresponded to the two equivalent orientations of the search model, were found when running the cross-rotation function. Since the space group is $P1$, the position of the molecule is arbitrary and a translation function was not required. An initial rigid-body refinement of the single $\alpha_2\beta_2$ tetramer in the crystallographic asymmetric unit was performed with *SHELX* (Sheldrick & Schneider, 1997), after which a number of amino-acid side chains were rebuilt using *TURBO FRODO* with $\sigma_{\rm A}$-weighted maps (Read, 1986). In further rounds of refinement two PQQ molecules, two calcium ions and 1405 water molecules were modelled into the electron density. The introduction of anisotropic displacement parameters and the use of riding H atoms using *SHELX* reduced the R factor and $R_{\rm free}$ to 15.8% and 19.6%, respectively. The final refinement and structure-quality statistics are shown in Table 1. The Ramachandran plot of the final structure shows that 86.6% of the residues are in the region most favoured by the *PROCHECK* criteria of Laskowski *et al.* (1993), with another 12.3% in the additionally allowed region, leaving four residues from the $\alpha_2\beta_2$ tetramer in disallowed regions; these were Lys19 and Asp105 from both of the α-subunits.

Table 1
Data-processing statistics and refinement statistics for the 1.2 Å resolution methanol dehydrogenase (MDH) structure.

Values in parentheses are for the outer resolution shell.

Total No. reflections collected	724568
No. unique reflections collected	373341
Resolution range for data collected (Å)	31.5–1.2 (1.26–1.20)
Completeness (%)	90.3 (80.2)
$R_{\rm merge}$ (%)	10.3 (44.2)
Multiplicity	2.0 (1.8)
Average $I/\sigma(I)$	4.4 (1.4)
Refinement resolution range (Å)	10.0–1.2
R factor (%)	15.8
$R_{\rm free}$ (%)	19.6
No. reflections in working set	353 944
No. reflections in test set	18 605
R.m.s. deviation from target bond lengths (Å)	0.020
R.m.s. deviation from target angle distances (Å)	0.045
R.m.s. distance from restrained planes (Å)	0.032
R.m.s. deviation from zero chiral volumes (Å^3)	0.067
R.m.s. deviation from target non-zero chiral volumes (Å^3)	0.068
R.m.s. deviation from target van der Waals contacts (Å)	0.166

3. Results and discussion

The overall structure of MDH from *Mb. extorquens* refined at 1.2 Å resolution is, as expected, very similar to the previously reported MDH structure, which was solved at an appreciably lower resolution (Ghosh *et al.*, 1995). The $\alpha_2\beta_2$ tetramer is arranged into two $\alpha\beta$ units, with the α-subunit exhibiting the eight-bladed β-propeller fold and the β-subunit wrapping around one side of the structure; the PQQ molecule is located at the centre of the β-propeller in each of the α-subunits. The improved resolution of the new data set allowed many surface polar side chains that had previously been poorly defined by the electron density to be positioned.

The atomic resolution data have allowed the PQQ conformation to be determined with no stereochemical restraints imposed during the refinement. This analysis has shown that the bound PQQ is a completely planar group and is probably in the oxidized orthoquinone form (Figs. 3 and 4). In contrast, the previously reported structure of MDH from *Mb. extorquens* possessed PQQ in the semiquinone oxidation state (Ghosh *et al.*, 1995). In this structure, the C-4 carbonyl atom of the orthoquinone moiety was distorted from planarity, exhibiting a 'kink' from the tricyclic plane of 40°. In spite of this difference, the hydrogen-bonding pattern of the PQQ moiety in the 1.2 Å structure is essentially the same as that in the previously reported analysis, showing only slight alterations in the geometry of the interactions. The planarity of the PQQ prosthetic group is consistent with a number of other recently solved quinohaemoprotein dehydrogenase structures (Chen *et al.*, 2002; Oubrie *et al.*, 2002).

The accuracy of the data has allowed a critical assessment of the nature of the metal ion in the active site. The calcium ion bound here forms an unusual coordination sphere in the active site. Three PQQ atoms coordinate to the calcium ion: these are the C-7 carboxylate, C-5 carbonyl O and N-6 quinoline N atoms. The remaining three calcium ligands are provided by both carboxylate O atoms from Glu177 and the O atom from the side chain of Asn261 (Fig. 3). The distances between the calcium ion and its coordinating atoms were reported to be between 2.3 and 2.8 Å in the earlier 1.9 Å resolution structure (Ghosh *et al.*, 1995). In the 1.2 Å resolution structure of MDH reported here, the bond length from the calcium ion to Asn261 is 3.18 Å (Fig. 3), suggesting that this side chain does not actually coordinate to the metal ion. However, Asn261 does hydrogen bond to the catalytic base Asp303 through its side-chain O atom (Afolabi *et al.*, 2001). This hydrogen bond serves to orient the Asp303 carboxylate group for an efficient proton abstraction from the substrate hydroxyl group in the initial step of the reaction.

Closer inspection of the $2F_{\rm o} - F_{\rm c}$ electron density occupied by the Ca^{2+} ion showed it to be oval rather than the expected spherical shape. Furthermore, some significant features of difference $F_{\rm o} - F_{\rm c}$ electron density were present. The enzyme

for this study was prepared from a methanol oxidation mutant that was defective in one of several processing enzymes that are required to either add the Ca^{2+} ion into the active site of MDH or remove an alternative metal ion in order to allow the Ca^{2+} ion to bind (Toyama *et al.*, 1998). Consequently, it was thought that the MDH preparation from this methanol oxidation mutant might contain Mg^{2+} (a far more abundant metal ion in cells) instead of Ca^{2+} in the active site. An Mg^{2+} ion was fitted to the electron-density maps for each of the two α-subunits in the asymmetric unit and the resulting model was refined using anisotropic *B* factors. Unfortunately, the refinement yielded very unsatisfactory electron density for the metal ions once Mg^{2+} was added into the structure. This result suggests that Mg^{2+} ions do not occupy the substrate-binding site.

Following this finding, a Ca^{2+} ion was re-inserted to replace the Mg^{2+} ion and the occupancy of the Ca^{2+} ion was refined during cycles of anisotropic *B*-factor refinement. The occupancy of the Ca^{2+} ion refined to 69% (the average of both α-subunits in the asymmetric unit) and its isotropic *B* factor was reduced from 30 to 20 Å^2. More importantly, the electron density surrounding the Ca^{2+} ion was more uniform and lacked any significant $F_o - F_c$ contribution. This fact led to the conclusion that in the crystals of MDH from the methanol oxidation mutant not all of the active sites are occupied by Ca^{2+} ions, suggesting a deficiency in the mechanism of metal insertion in these mutant bacteria.

The unusual disulfide bridge formed between adjacent cysteine residues Cys103 and Cys104 has recently been implicated in intramolecular electron-transfer events in the quinohaemoprotein alcohol dehydrogenases from *C. testosteroni* (Chen *et al.*, 2002) and *P. putida* (Oubrie *et al.*, 2002). Quinohaemoprotein alcohol dehydrogenases are type II PQQ-containing alcohol dehydrogenases. This class of redox proteins are periplasmic proteins that contain both a PQQ-containing domain, folded into a β-propeller fold, and a smaller cytochrome *c* domain, which is analogous to a typical class I *c*-type cytochrome. These two domains are connected *via* a proline-rich linker region, which lacks any secondary structure, and we have used these structures to model the electron-transfer complex formed by MDH and cytochrome c_L.

The X-ray crystal structures of the quinohaemoprotein dehydrogenases (Chen *et al.*, 2002; Oubrie *et al.*, 2002) have allowed speculative electron- and proton-transfer pathways from the PQQ domain to the cytochrome *c* domain to be postulated. These pathways have highlighted various water molecules and protein residues as being crucial to this process. After comparing the active site of MDH with the quinohaemoproteins, it was apparent that the majority of the components of these postulated pathways for proton and electron transfer were conserved, making the quinohaemoprotein alcohol dehydrogenases a good model for the MDH–

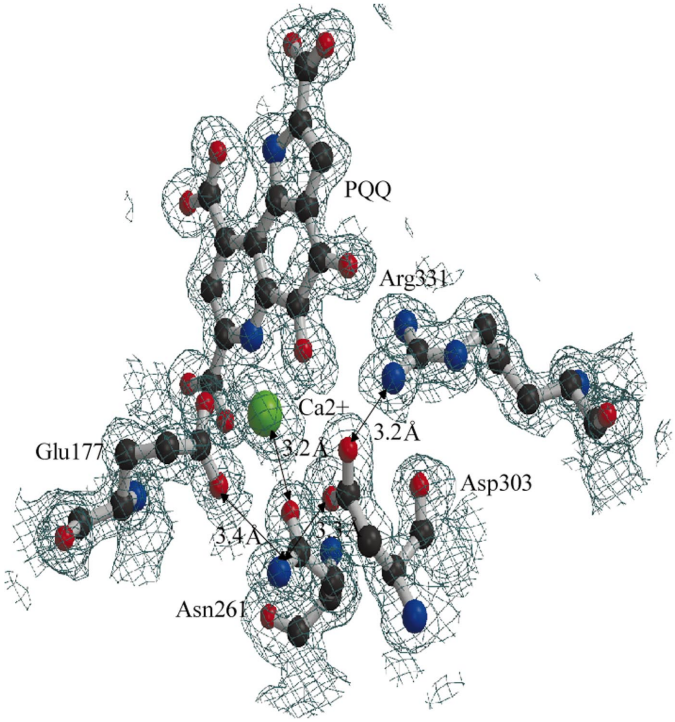

Figure 3
The interactions made by the active-site Ca^{2+} ion. The length of the interaction between Asn261 and the Ca^{2+} ion is 3.18 Å, which is too long to be considered a coordinated bond. The 1.2 Å resolution $2F_o - F_c$ map contoured at the 1.0σ level is shown in grey/blue lines.

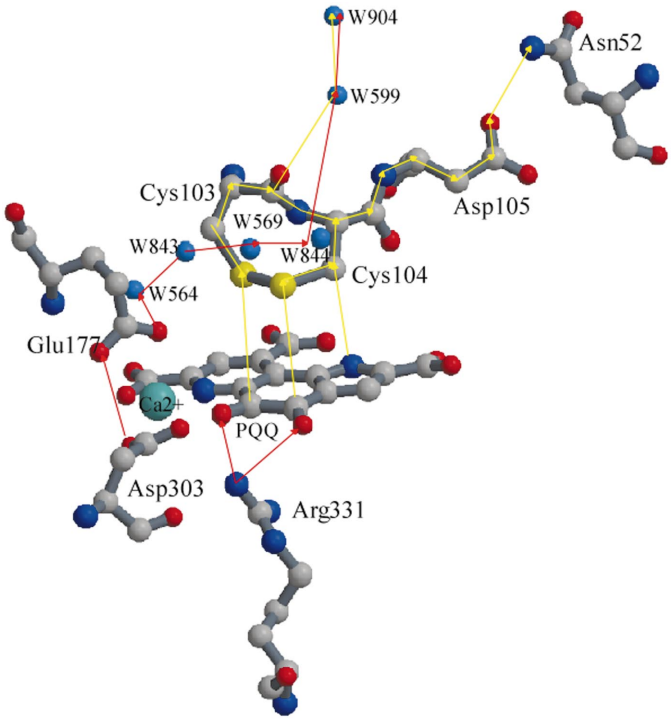

Figure 4
Proposed pathways for electron transfer from PQQ to cytochrome c_L (shown in yellow) and proton translocation from PQQ to the periplasm (shown in red). Both pathways are predicted on the basis of the structures of the quinohaemoprotein alcohol dehydrogenase from the bacterium *C. testosteroni* (Oubrie *et al.*, 2002). The electrons originating from oxidation of methanol would travel from the PQQ cofactor into the adjacent disulfide and then towards Asn52 or the water molecules 599 and 904 and thence to cytochrome c_L. The putative proton-transfer pathway involves the side chains of a number of acidic and basic residues as well as active-site water molecules.

cytochrome c_L interaction. Amongst these features were the disulfide bond formed between Cys103 and Cys104, Asp105 and a channel of water molecules, which constitute a solvent channel leading from the PQQ molecule to the surface of MDH, where a cytochrome c_L molecule could bind and accept an electron. A potential pathway for the electron to reach the protein exterior is shown in Fig. 4 (yellow arrows). The release of protons from the catalytic site to the surrounding periplasm establishes a proton gradient across the periplasmic membrane. A number of residues that are likely proton-transfer candidates are shown in Fig. 4 (red arrows). The proton-transfer pathway is thought to involve the side chains of a number of acidic and basic residues, as well as water molecules held within the active-site cleft. In conclusion, we believe that this is an interesting example of how knowledge of the structure of a two-domain protein can be used to model the functional complex formed by two proteins, each homologous with one domain of the 'parent' structure.

The authors gratefully acknowledge the Biotechnology and Biological Sciences Research Council (UK) for project grant support and a research studentship (to PAW). The authors also thank the European Synchrotron Radiation Facility (ESRF, Grenoble) for provision of beam time and associated travel support.

References

Afolabi, P. R., Mohammed, F., Amaratunga, K., Majekodunmi, O., Dales, S. L., Gill, R., Thompson, D., Cooper, J. B., Wood, S. P., Goodwin, P. M. & Anthony, C. (2001). *Biochemistry*, **40**, 9799–9809.
Anthony, C. (1992). *Biochim. Biophys. Acta*, **1099**, 1–15.
Anthony, C. (2004). *Respiration in Archaea and Bacteria*, Vol. 1, *Diversity of Prokaryotic Electron Transport Carriers*, edited by D. Zannoni, pp. 203–225. Dordrecht: Kluwer Academic Publishers.
Brünger, A. T. (1992). *Nature (London)*, **355**, 472–474.
Chen, Z. W., Matsushita, K., Yamashita, T., Fujii, T., Toyama, H., Adachi, O., Bellamy, H. D. & Mathews, S. F. (2002). *Structure*, **10**, 837–849.
Collaborative Computational Project, Number 4 (1994). *Acta Cryst.* D**50**, 760–763.
Dijsktra, M., Frank, J. & Duine, J. A. (1989). *Biochem. J.* **257**, 87–94.
Ghosh, M., Anthony, C., Harlos, K., Goodwin, M. J. & Blake, C. C. F. (1995). *Structure*, **3**, 177–187.
Laskowski, R. A., MacArthur, M. W., Moss, D. S. & Thornton, J. M. (1993). *J. Appl. Cryst.* **26**, 283–291.
Leslie, A. G. W. (1992). *Jnt CCP4/ESF–EACBM Newsl. Protein Crystallogr.* **26**.
Oubrie, A., Rozeboom, H. J., Kalk, K. H., Huizinga, E. G. & Dijkstra, B. W. (2002). *J. Biol. Chem.* **277**, 3727–3732.
Read, R. J. (1986). *Acta Cryst.* A**42**, 140–149.
Read, J., Gill, R., Dales, S. L., Cooper, J. B., Wood, S. P. & Anthony, C. (1999). *Protein Sci.* **8**, 1232–1240.
Sheldrick, G. M. & Schneider, T. R. (1997). *Methods Enzymol.* **277**, 319–343.
Toyama, H., Anthony, C. & Lidstrom, M. E. (1998). *FEMS Microbiol. Lett.* **166**, 1–7.
Vagin, A. & Teplyakov, A. (1997). *J. Appl. Cryst.* **30**, 1022–1025.
Xia, Z. X., He, Y. N., Dai, W. W., White, S. A., Boyd, G. D. & Mathews, F. S. (1999). *Biochemistry*, **38**, 1214–1220.